Available online at www.sciencedirect.com
ScienceDirect
Journal of Power Sources 179 (2008) 631–639
JOURNAL OF POWER SOURCES
www.elsevier.com/locate/jpowsour

Bipolar plate materials for PEMFCs: A conductivity and stability study

A. Pozio *, F. Zaza, A. Masci, R.F. Silva

ENEA, C.R. Casaccia, Via Anguillarese 301, 00123 S. Maria di Galeria, Rome, Italy

Received 28 November 2007; received in revised form 7 January 2008; accepted 19 January 2008
Available online 1 February 2008

Abstract

Commercial stainless steels, Ni-based alloys and physical vapor deposition (PVD) chromium nitride (CrN)-coated stainless steels were evaluated as possible metallic bipolar plate materials in conditions that resemble a typical PEMFC cathode environment with respect to their interfacial contact resistance (ICR) and corrosion resistance. Results show that stainless steels have a high ICR and undergo corrosion. Although Ni-based alloys showed an ICR value comparable as to that of graphite, their behaviour was not satisfactory in a corrosive acidic medium. Only CrN-coated stainless steels demonstrated to have low ICR values and a very good corrosion resistance.
© 2008 Elsevier B.V. All rights reserved.

Keywords: CrN; Stainless steels; Ni-based alloys; PVD; Contact and corrosion resistances; PEMFC

1. Introduction

Polymer electrolyte membrane fuel cells (PEMFCs) are devices that convert the chemical energy of a fuel directly into electrical energy and thus are very promising as an energy source thanks to their high power density performance at low temperature (70–90 °C) [1]. Unlike the internal combustion engine there is no burning of the fuel and therefore no generation of pollutants. Since a single cell can only give an output voltage around 0.5–0.7 V, the cells are stacked together in series, connected by means of bipolar plates.

The bipolar plates are a multifunctional component in PEMFC stacks as they collect and conduct the current from cell to cell, they separate the gases, and the flow channels in the plates deliver the reacting gases to the fuel cell electrodes [2]. In a typical fuel cell stack, the bipolar plates comprise over 80% of the mass, and almost all of the volume. In the absence of dedicated cooling plates, the bipolar plates also facilitate heat management. The most widely used bipolar plate materials are the graphite-based composites, which are ideal in terms of corrosion resistance and conductivity [3,4]. Nevertheless, their high cost and the need for machining to form the flow channels limit these materials for applications involving high-volume manufacturing. In addition, graphite composites lack mechanical strength, and therefore the thickness of the plates cannot be reduced. This results in thicker plates with bulkier sizes and more elevated weights. Due to these problems, alternative materials suitable for use in fuel cell technology and able to achieve long lifetime are a key issue in this research field. Several alternatives to the machining of graphite sheets have been investigated including: compression and injection moulding of graphite-filled polymer [5], carbon–carbon composite materials [6] and carbon–polymer composite materials [7]. Metals can also be used to make bipolar plates, and have the advantages of being very good heat and electricity conductors, can be machined easily (e.g. by stamping), are non-porous, and consequently very thin pieces will serve to keep the reactant gases apart. The major disadvantage of metals is that they are prone to corrosion and passivation. A possible solution to avoid this disadvantage is the use of corrosion resistant materials like stainless steels (SSs). Many works have been devoted to broaden the application of 304, 316L, 349^{TM}, 446, and 904L stainless steels in weakly acidic media in order to overcome the insufficient corrosion resistance [8–13]. The results are in accordance with the fact that the common stainless steels show an increase of the contact resistance in a short period of time

* Corresponding author. Tel.: +39 06 3048 4071; fax: +39 06 3048 6357.
E-mail address: alfonso.pozio@casaccia.enea.it (A. Pozio).

0378-7753/$ – see front matter © 2008 Elsevier B.V. All rights reserved.
doi:10.1016/j.jpowsour.2008.01.038

and also undergo a loss of material in the operative conditions of a PEMFC [14]. Two possible alternatives for stainless steel bipolar plates are Ni-based alloys [15–21] or a physical vapor deposition (PVD) coated stainless steel [22,23] in order to protect the metal bipolar plates and to lower the contact resistance. As shown in previous works [24,25], common stainless steels demonstrated to be unsuitable because of the presence of a passive layer with a low conductivity due to the presence of non-conductive oxides, leading to high interfacial contact resistance (ICR) values. Ni-based alloys showed much lower ICR values due to a lower [Fe + Cr] amount. In addition, all the Ni-based alloys have an ICR value lower than that of BMA5 graphite (SGL Germany). In particular, the ICR of C-276® is also lower than that of the best commercially available XM9612 graphite (SGL Germany). Chromium nitride (CrN) coated stainless steel specimens presented a lower ICR value than that of the best uncoated 904L stainless steel. In addition, endurance tests in cathode and anode environments gave very promising results. Long-term stability tests in a single fuel cell were demonstrated for a PVD nitride-coated SS304 sample [25].

In this work, the ICR of three groups of alloyed materials, namely Ni-based alloys (Nicrofer® hMo 3127®, 6020® and 5923®), PVD CrN-coated SS316L or SS304, and common 316L or 304 stainless steel are compared with that of graphite material. All the materials are examined in terms of their ICR in oxidizing conditions typical of a PEFMC environment. The corrosion current density of the specimens in both anode and cathode conditions is also evaluated at room temperature.

2. Experimental

2.1. Materials

The austenitic stainless steel specimens SS316L were provided by Ulbrich Stainless Steels (USA) and SS304 was provided by Metinox (Italy). Nicrofer® hMo 3127®, 6020® and 5923® Ni-based alloys were provided by ThyssenKrupp Stainless. The typical chemical compositions of the stainless steels investigated in this work are given in Table 1. The specimens were cut into pieces of about 16 cm^2, polished with #600 grit SiC abrasive paper and cleaned with ethanol and distilled water.

Polished pieces of SS316L and SS304 were coated by means of the PVD process with a CrN layer from Genta Platit (Ferioli & Gianotti S.p.A Groups, Italy). Two commonly used materials for bipolar plates (XM9612 and BMA5 graphites) were purchased from SGL Carbon Group (Germany) and used as reference.

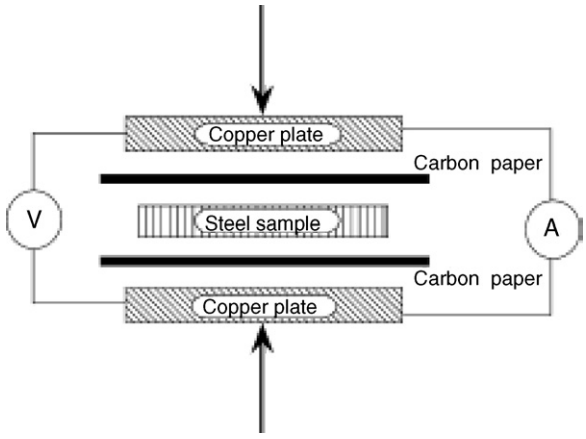

Fig. 1. Schematic illustration of the test assembly for the ICR measurements.

2.2. Interfacial contact resistance

In order to obtain optimized parameters for the cell assembly, the original method of Davies et al. [10] was used following the modifications done by Wang et al. [11] and Lee et al. [19,20] for the ICR measurements between stainless steel and carbon paper. In our setup, two pieces of conductive carbon paper (Toray TGPH090) were sandwiched between the sample and two copper plates (Fig. 1). The contact resistance was obtained by means of a Burster mod. 2318 milli-ohmmeter. The device operates with the principle of the four-wire current–voltage measurement eliminating transition and lead resistances. The potential difference (V) across the cell was measured whilst a fixed electrical current (I) was passed through the arrangement. The current applied was in the range of 90–900 mA. The compaction force was gradually increased with the use of an ATS FAAR (Italy) hydraulic press monitored by means of a Unomat mod. MCX pressure controller.

The total measured resistivity losses directly obtained according to the relation $R = V/I$ can be used to calculate the ICR of all the specimens by means of the following equation:

$$\mathrm{ICR} = \frac{(R - R_{\mathrm{CP}})}{2} \times A \quad (1)$$

where R_{CP} represents the resistive contribution due to the carbon paper/copper interface; the resistance is 3.3–11 mΩ in the range of compaction pressure 1–340 N cm^2, and A is the specimen area.

Table 1
Chemical composition (wt.%) of stainless steels and Ni-based alloys by EDX analysis

Alloy/UNS	Cr	Mo	Ni	Al	Nb	Ta	Cu	Fe	Others
SS316L-S31603	17.0	2.1	8.9	–	–	–	–	71.8	0.2
SS304/S30400	17.6		7.2					75.0	0.2
Nicrofer®-3127 hMo	27.3	11.0	28.1	–	–	–	1.0	32.2	0.4
Nicrofer®-6020 hMo	20.5	9.3	60.0	1.0	3.8	1.5	–	3.3	0.6
Nicrofer®-5923 hMo	22.3	21.5	54.5	–	–	–	–	0.9	0.7

As reference, the ICR of the two commercially available SGL graphites (XM9612 and BMA5) typically used as material for bipolar plates was measured. A comparison with the results from the literature [3,17,20] showed that the ICR was greatly affected by the compaction force and that a good reproducibility can be obtained only above 150 N cm^{-2}. The ICR was measured on the as-received specimens and also on the same specimens submitted to corrosion endurance tests, as explained in the following section.

2.3. Electrochemical measurements

Corrosion endurance tests were done to simulate the aggressive PEMFC environment [11,20]. Specimens of the above-listed materials were placed in a corrosion cell with an exposed area of 4.52 cm^2. Experiments were carried out in a 10^{-3} M $H_2SO_4 + 1.5 \times 10^{-4}$ M HCl + 15 ppm HF solution at a variable temperature of 25–70 °C. The corrosion cell was immersed in a thermostatic bath (Haake). The temperature was changed from 25 °C (night) up to 70 °C in the working hours and it was decreased to 25 °C in the weekends. During the test, air was bubbled continuously to simulate the cathode environment. A saturated calomel electrode (SCE) connected to a Luggin capillary served as the reference electrode and a platinum sheet as the counter electrode. The potential values are reported with reference to the normal hydrogen electrode (NHE). All the measurements were performed using a Solartron 1287 potentiostat and the CorrWare 2.1 software (Scribner Inc.). The open-circuit potential (OCP) was measured during the experiments for a total period of approximately 220 h (about 64 h at 70 °C).

Polarization curves were also obtained for different specimens sparging the solution with hydrogen gas or air. At the beginning of each experiment, the working electrode was cathodically polarized at −0.759 V versus NHE for 5 min to remove surface oxides and to assure reproducibility. Then the corrosion potential (E_{corr}) at OCP was measured for 1 h and polarization curve determinations were conducted in the range from −0.309 to 0.941 V versus NHE at a scan rate of 0.33 mV s^{-1}. The linear polarization method was employed for uniform corrosion evaluation [19].

2.4. Surface analysis

Scanning electron microscopy (SEM) was used to investigate the morphology of the as-received specimens as well as those submitted to corrosion endurance tests. All the micrographs and energy dispersive X-ray (EDX) spectra were acquired with a JEOL mod. JSM5510LV scanning electron microscope and an IXRF/500 accessory, respectively.

The crystal structure of the nitrited layers was investigated with a Rigaku Miniflex diffractometer. The patterns were obtained using a Cu Kα radiation from a rotating anode source operating at 30 kV and 15 mA. The specimens were scanned at 0.02° s^{-1} in the continuous scan mode over the 2θ range 30–100°.

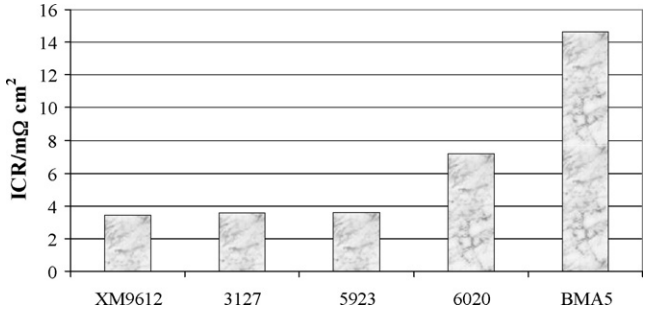

Fig. 2. Interfacial contact resistance (bars) at the compaction force of 220 N cm^{-2} of Nicrofer® 3127, 6020® and 5923®, and BMA5 and XM9612 graphites.

3. Results and discussion

3.1. ICR experiments

In the first experiments of this work we tested the ICR versus the compaction force of all materials (Nicrofer® hMo 3127®, 6020®, and 5923®) in order to make a comparison with two types of SGL graphite (BMA5 and XM9612). Fig. 2 shows the results at the typical compaction force of a single cell (220 N cm^{-2}) [10]. This result agrees with the trend already observed in previous work for other commercial alloys (SS304, SS310, SS316 904L) and Ni-based alloys (G-30®, C-2000B®, C-22®, and C-276®) [24]. In fact, previous results [24,25] evidenced high ICR values (50–90 mΩ cm^2) for conventional commercial steel (SS304, SS310, SS316L, 904L) with respect to that of commonly used graphites and Ni-based alloys. Also in this case, the ICR of the Ni-based alloys is always lower than that of the BMA5 graphite and quite similar to that of XM9612 graphite (BMA5 > 6020® > 5923® = 3127® > XM9612). The influence of chromium oxide on the Fe- and Ni-based material resistance is very complex [26]. In fact, oxides can have conductor, semiconductor or insulator features simply by varying their stoichiometric composition and/or by doping with other elements. Generally, it can be considered that among the oxides the decrease of conductivity follows the trend Ni-oxide > Cr-oxide > Fe-oxide. Previously, we related the ICR of Ni-based alloys to the chromium and iron content in the stainless steel [24], as these constituents have the major impact on the thickness of the passive film. Taking the composition data from Table 1, the [Fe + Cr] trend is SS316L ≫ 3127® > 6020® > 5923®.

In this case we observe a discrepancy with the trend previously observed on other Ni-based alloys [24,25], particularly for the 3127® that has a high Fe amount but a very low ICR. As an explanation, we can consider that the 3127® is a very particular stainless steel characterized by nitrogen addition. The use of nitrogen in the austenitic stainless steel favours the occurrence of various chromium nitrides of which Cr_2N is the most common. The presence of nitrogen, a strong austenitic former, remarkably increases the resistance to pitting and crevice corrosions, as can be observed by the pitting resistance equivalent number (PREN) defined for austenitic steel as [8,27]

$$\mathrm{PREN} = \mathrm{Cr\%} + 3.3\%\,\mathrm{Mo} + k\%N \quad (2)$$

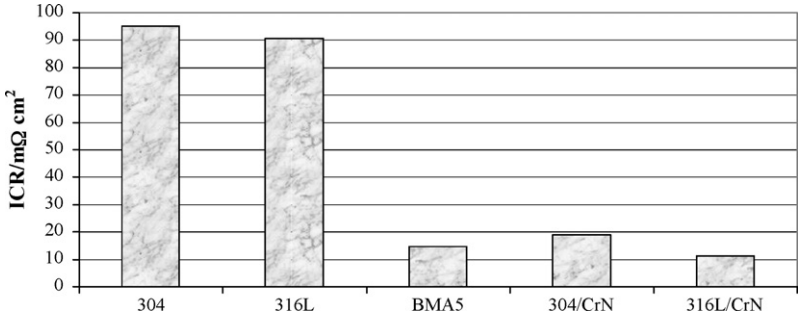

Fig. 3. Interfacial contact resistance at the compaction force of 220 N cm^{-2} of as-received SS316L, SS304 specimens and PVD-coated SS304/CrN, SS316L/CrN specimens.

The last term in Eq. (2) takes into account the nitrogen addition, where k is reported to be 16 or 30. This equation indicates that the resistance of stainless steel to pitting corrosion increases as the proportion of these alloying elements is increased, but the influence of nitrogen is 16 times higher than that of chromium content and ~5 times higher than that of Mo. In order to explain the trend observed for the ICR values, the effect of other alloying elements like Nb, Ta, Al and Cu should be evaluated. However, preliminary results allow us to exclude the possibility of using these commercial Ni-based alloys.

With regard to the specimens SS316L/CrN and SS304/CrN, Fig. 3 reports the ICR values of coated samples compared with uncoated SS316L and SS304. A marked decrease of ICR (−88% and −80%) was observed for the two CrN-coated samples with respect to the bare steel, which is comparable with that of graphite. Nitridation of Ni-50Cr by arc casting on a special austenitic 349^{TM} stainless steel was studied by Wang et al. [21] who obtained a reduction of the interfacial contact resistance together with a poor behaviour in terms of corrosion. Generally, the 349^{TM} was characterized by a lower ICR than that of common SS304 and SS316 due to a higher load of Ni (14.5%) and the presence of both Nb, a strong carbide and nitride former, and nitrogen [11].

Table 2
ICR at 150 N cm^2 for CrN-coated stainless steel specimens

Samples	ICR (mΩ cm^2)	Method	Authors
SS316/CrN	21	PVD-coated	This work
SS304/CrN	30	PVD-coated	This work
SS349^{TM}/CrN	10	Thermally nitrided	[21]
SS316/CrN	50	Thermally nitrided	[28]

Nam and Lee [28] attempted the thermal nitridation of an electroplated chromium layer on AISI316L stainless steel obtaining an ICR value of an order of magnitude lower than that of bare AISI316L stainless steel. Table 2 compares the ICR values obtained from various authors for this type of coating at 150 N cm^2. Results are similar, but clearly the difference of bare and coated materials plays a determining role in the resulting interfacial contact resistance. In all these works a good result seems to be related to the formation of a stable, non-porous, conductive CrN layer able to decrease the ICR and protect the bare steel from corrosion. In any case, the PVD coating of CrN directly onto bare steel appears as a simpler method than the nitridation of electro- or arc-melt deposited chromium layers.

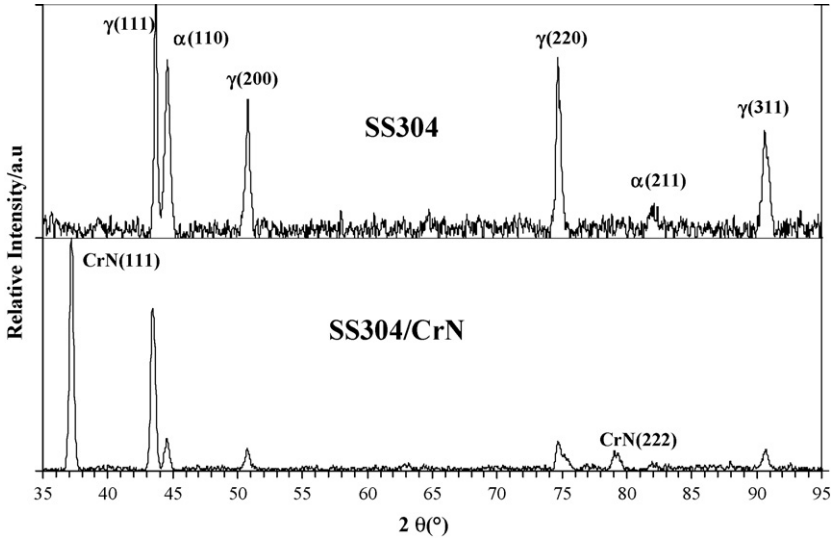

Fig. 4. XRD patterns of as-received SS304 and PVD-coated SS304/CrN specimens.

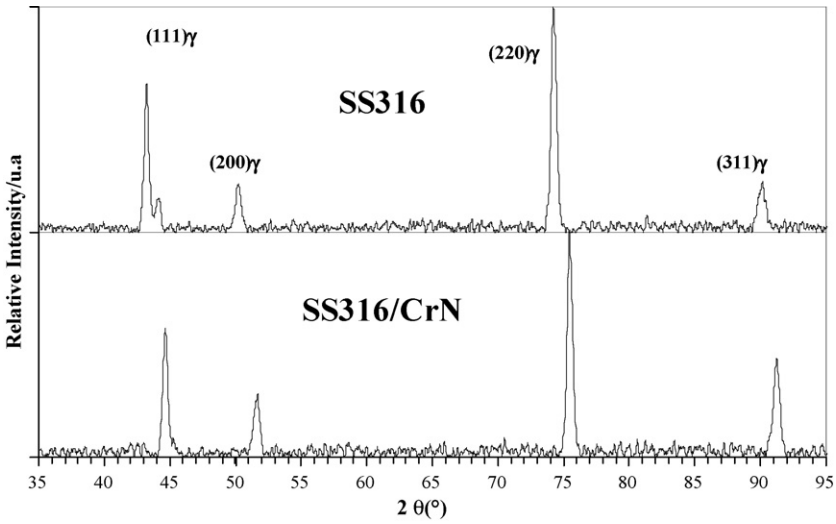

Fig. 5. XRD patterns of as-received SS316L and PVD-coated SS316L/CrN specimens.

The X-ray diffraction analyses for the SS304-SS304/CrN and SS316L-SS316L/CrN specimens are depicted in Figs. 4 and 5. As already observed for untreated SS304 and SS316L specimens, we notice the presence of the martensitic Fe(α) and the austenitic Fe(γ) phases where the first is related to a mechanical polishing effect [29]. The SS304/CrN steel shows a well-defined CrN(1 1 1) peak at about 37° and a low-intensity CrN(2 2 2) peak at 79° evidencing a crystalline coating [22]. Conversely, SS316L/CrN does not present any CrN peak, which suggests a porous (or non-crystalline) CrN coating confirmed also by the ICR results presented in the following section.

3.2. Cathode characterization

On the basis of the above results, the Ni-based alloys 3127®, 5923® and 6020®, and the stainless steels SS304 – SS304/CrN and SS316 – SS316/CrN were selected for comparative endurance tests. During the experiment, air was bubbled continuously to simulate the cathode environment. The results in Fig. 6 show the ICR values before and after the tests. Before realization of the endurance test, all the Ni-based alloys presented very low ICR values, which increased by a factor of 21–25 after the corrosion treatment, thus contrasting with the SS304/CrN whose interfacial contact resistance remained unchanged. Such results confirm those obtained for the Ni-based alloy C-276® [24,25] that also had the ICR increased by a factor of 25.

The SS316/CrN specimen also showed an initial ICR value lower than that of uncoated SS316. However, due to the porous nature of the CrN coating, the value increased about six times after the corrosion treatment. Further analyses are necessary to define an exact procedure for the CrN coating on this kind of steel.

The SEM microscopy was used to study the morphology of the investigated specimens before and after the endurance tests. A micrograph of the best-performing Ni-based alloy 3127® specimen is shown in Fig. 7, where it can be verified the presence of pitting corrosion not widely distributed on the sample surface with holes having a diameter of approximately 15–20 μm. On the other hand, the morphological analysis of the SS304/CrN specimen indicates the absence of precipitate formation and pitting corrosion (Fig. 8). Before the endurance test, the SS316L/CrN specimen revealed the presence of a coat-

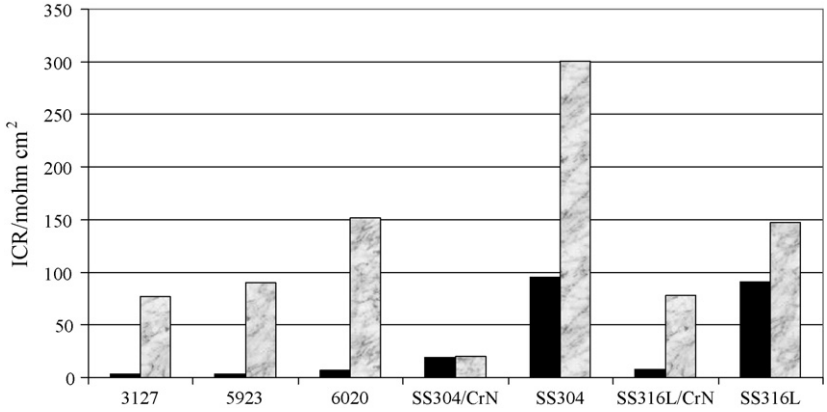

Fig. 6. Interfacial contact resistance at the compaction force of 220 N cm^{-2} before and after corrosion endurance tests of Nicrofer® 3127, Nicrofer® 6020, Nicrofer® 5923, SS304, SS304/CrN, SS316L and SS316L/CrN specimens.

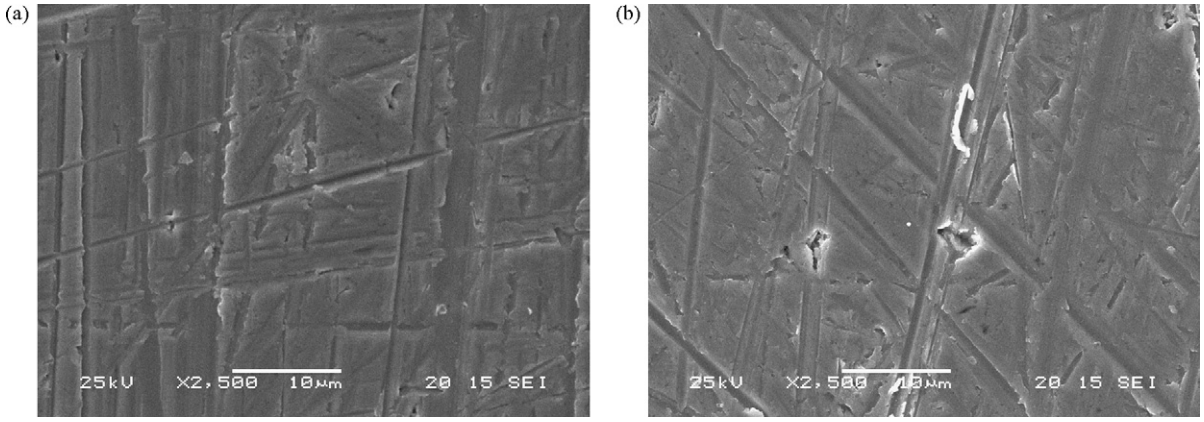

Fig. 7. SEM micrographs of a Nicrofer® 3127 specimen before (a) and after (b) 220-h corrosion endurance test.

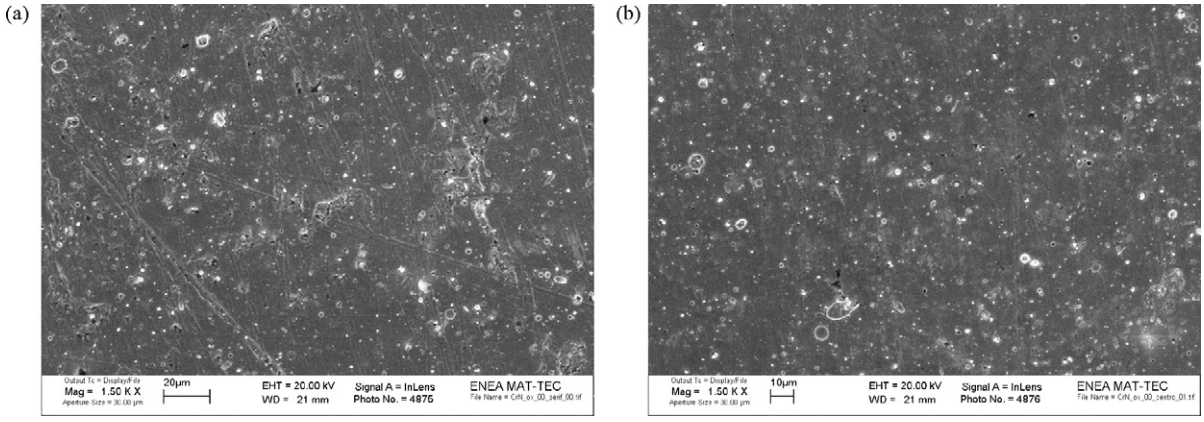

Fig. 8. SEM micrographs of a SS304/CrN specimen before (a) and after (b) 220-h corrosion endurance test.

ing having holes with a diameter of approximately 15–20 μm (Fig. 9a). After the endurance test, it was verified a localized corrosion particularly on the grain border near the holes (Fig. 9b–d).

All the specimens were also compared by means of potentiodynamic experiments in simulated cathode environment to estimate the characteristic corrosion current of each analysed material. The results for the cathodic condition shown in Table 3 evidence a decrease of the corrosion current density, and the current at 0.7 V versus NHE for the CrN-coated samples compared to bare SS316L and SS304 and all the Ni-based alloys.

In more details, SS304 was characterized by a very short passivation zone and by a high anodic current (Fig. 10). In addition, an anodic current peak is present at about 0.71 V versus NHE (6.4×10^{-6} A cm^{-2}). On the other hand, the SS304/CrN specimens showed an anodic current about five times lower than that of the bulk SS304 specimen. Despite the different corrosion potential, which is probably related to the surface composition, these results fit well with the ICR measurements before and after the endurance test (Fig. 6) and attest for a promising performance of this coating in the cathode environment.

Ni-based alloy specimens were all characterized by an extended passivation range (0.50–0.75 V vs. NHE), and their corrosion current was found to be similar to that of the conventional stainless steels (SS304 and SS316) (Fig. 11). Also very interesting are the SS316L/CrN specimens characterized by both an extended passivation range and a corrosion current about 2.2–8.7 lower than that of the bulk SS316 specimen (Fig. 12).

Table 3
Corrosion current density, corrosion potential and current density at 0.7 V vs. NHE

Samples	i_{corr} (μA cm^{-2})	E_{corr}/V vs. NHE	I (μA cm^{-2}) at 0.7 V
SS304	0.48	0.56	3.26
SS304/CrN	0.10	0.84	0.24
SS316L	0.46	0.14	1.92
SS316L/CrN	0.20	0.15	0.79
Nicrofer®-3127 hMo	0.24	0.25	3.14
Nicrofer®-6020 hMo	0.83	0.19	4.97
Nicrofer®-5923 hMo	0.49	0.17	1.95

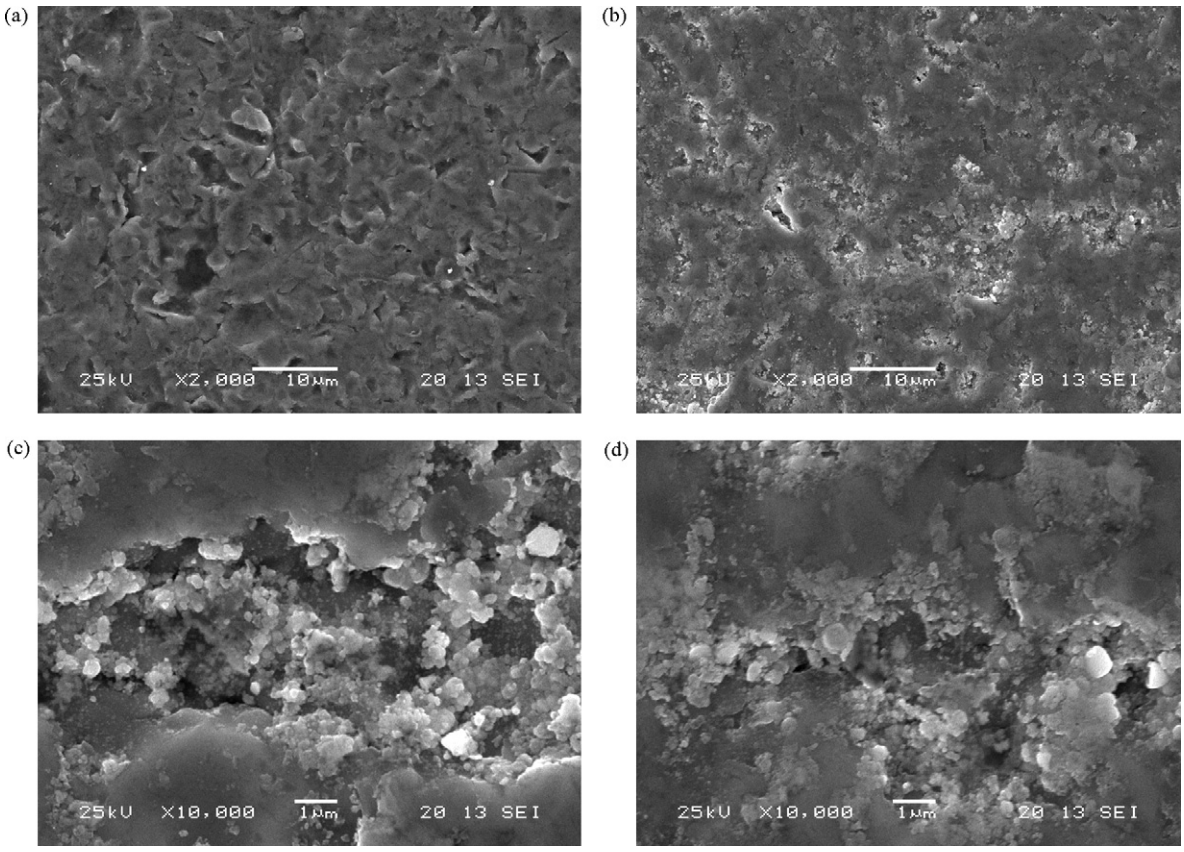

Fig. 9. SEM micrographs of SS316L/CrN specimen before (a) and after (b–d) 220-h corrosion endurance test.

3.3. Anode characterization

SS304/CrN and SS304 specimens were also compared in anodic conditions. Fig. 13 shows the ICR values of the specimens before and after corrosion in a solution bubbled with hydrogen. An increase of the corrosion resistance for both specimens can be observed, although the ICR value of the SS304/CrN remained under 25 $m\Omega\,cm^2$.

Fig. 14 shows the potentiodynamic curves of the SS304/CrN specimen compared with bare SS304. It can be noticed that the specimens are characterized by much lower corrosion potentials than the potentials obtained in the cathode environment. The SS304 specimen has a corrosion potential ($E_{corr} = -0.184$ V vs. NHE) lower than that of the CrN-coated specimens ($E_{corr} = -0.067$ vs. NHE). The trend observed for the corrosion current is SS304 ($i_0 = 2.5\ \mu A\,cm^{-2}$) > SS304/CrN ($i_0 = 0.22\ \mu A\,cm^{-2}$); although the CrN-coated stainless steel has a lower corrosion current, the current value found is higher than those registered in the cathode environment. Also, these results fit well with the ICR measurements before and after

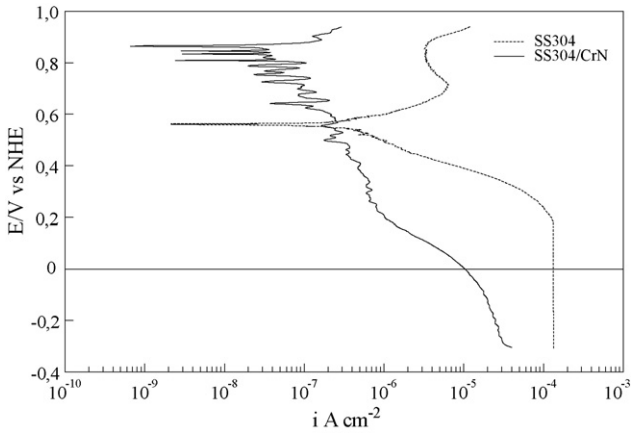

Fig. 10. Polarization curves at 0.33 mV s^{-1} of SS304 and SS304/CrN specimens in a 10^{-3} M $H_2SO_4 + 1.5 \times 10^{-4}$ M + 15 ppm HF solution purged with air at 25 °C.

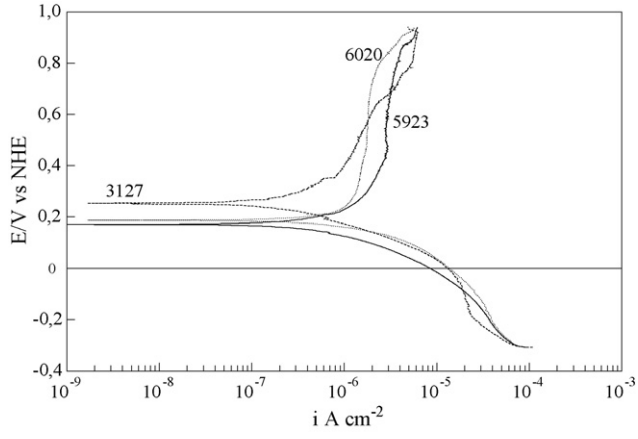

Fig. 11. Polarization curves at 0.33 mV s^{-1} of Nicrofer® 3127, 6020®, and 5923® specimens in a 10^{-3} M $H_2SO_4 + 1.5 \times 10^{-4}$ M + 15 ppm HF solution purged with air at 25 °C.

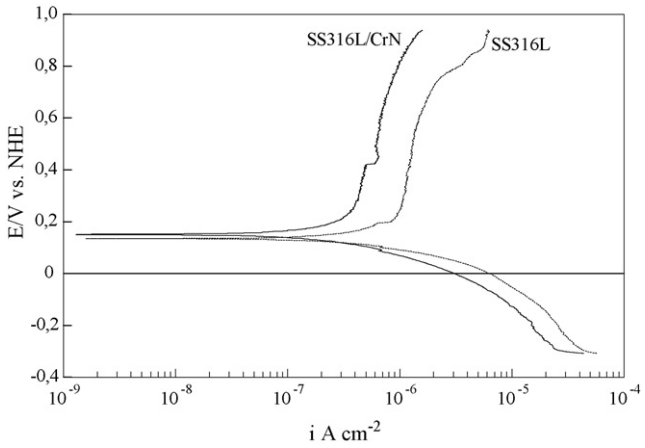

Fig. 12. Polarization curves at 0.33 mV s^{-1} of SS316L, SS316, Nicrofer® 3127, Nicrofer® 6020, and Nicrofer® 5923 specimens in a 10^{-3} M $H_2SO_4 + 1.5 \times 10^{-4}$ M + 15 ppm HF solution purged with air at 25 °C.

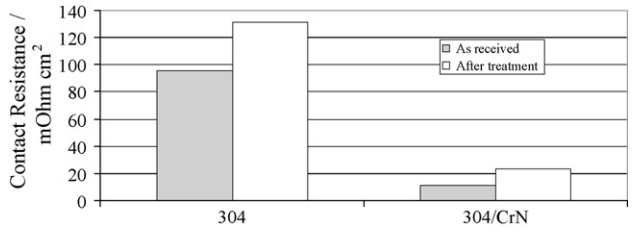

Fig. 13. Interfacial contact resistance at the compaction force of 220 N cm^{-2} before and after corrosion endurance test for SS304 and SS304/CrN specimens.

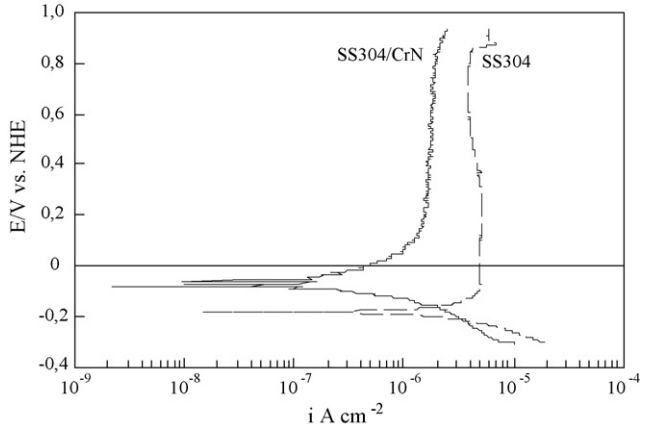

Fig. 14. Polarization curves at 0.33 mV s^{-1} of SS304 and SS304/CrN specimens in a 10^{-3} M $H_2SO_4 + 1.5 \times 10^{-4}$ M + 15 ppm HF solution purged with H_2 at 25 °C.

the endurance test in anodic environment. A higher corrosion current does not imply a high ICR, especially in the anode environment. Constituent may go into solution leaving a bare surface showing a low ICR. In this case, as in the cathode environment, a high corrosion current implies a higher rate for ICR increase.

4. Conclusion

Low-cost common stainless steel, Ni-based alloy and PVD CrN-coated stainless steel specimens were tested as alternative materials for PEMFC bipolar plates and compared with two kinds of reference graphite in terms of interfacial contact resistance and corrosion resistance. Common stainless steels demonstrated to be unsuitable because of the presence of too large amount of non-conductive oxide (e.g. [Fe + Cr] > 69% and Ni < 24%) that leads to high ICR values. Ni-based alloys showed much lower ICR values due to a lower [Fe + Cr] amount. In addition, all the Ni-based alloys have an ICR value lower than that of BMA5 graphite, and particularly the ICRs of 3127® and 5923® are also lower than that of best-performing commercially available XM9612 graphite. The coated stainless steel specimens SS304/CrN and SS316/CrN presented a lower ICR value with respect to that of the bulk materials. In addition, endurance tests in cathode and anode environments gave very promising results especially for the SS304/CrN. In this sense, the PVD method can represent an interesting alternative for bipolar plate manufacturing. An investigation is being conducted by our group in order to analyse the optimal composition and thickness for the SS316/CrN specimen and then to evaluate long-term stability tests in a single fuel cell. The fact that the SS316/CrN does not yield similar results as the coated SS304 due to an imperfect coating shows the weak point of coated stainless steels for use in a PEMFC, i.e. the coating should be completely defect free. Further analysis of the corrosion layers prior and after the immersion tests are necessary in order to explain the large increase in the ICR of the Ni-based alloys.

References

[1] S. Gottesfeld, T. Zawodzinski, Adv. Electrochem. Sci. Eng. 5 (1997) 195.
[2] V. Mehta, J.S. Cooper, J. Power Sources 114 (2003) 32.
[3] P.L. Hentall, J.B. Lakeman, G.O. Mepsted, P.L. Adcock, J.M. Moore, J. Power Sources 80 (1999) 235.
[4] J. Scholta, B. Rohland, V. Trapp, U. Focken, J. Power Sources 84 (1999) 231.
[5] A. Heinzel, F. Mahlendorf, O. Niemzig, C. Kreuz, J. Power Sources 131 (1/2) (2004) 35.
[6] T.M. Besmann, J.W. Klett, J.J. Henry Jr., E. Lara-Curzio, J. Electrochem. Soc. 147 (2000) 4083.
[7] D.N. Busick, M.S. Wilson, Fuel Cell Seminar, Palm Springs, 1998, (Abstract 1186).
[8] R. Hornung, G. Kappelt, J. Power Sources 72 (1998) 20.
[9] R.C. Makkus, A.H.H. Janssen, F.A. de Brujin, R. Mallant, J. Power Sources 86 (2000) 274.
[10] D.P. Davies, P.L. Adcock, M. Turpin, S.J. Rowen, J. Power Sources 86 (2000) 237.
[11] H. Wang, M.A. Sweikart, J.A. Turner, J. Power Sources 115 (2003) 243.
[12] H. Wang, J.A. Turner, J. Power Sources 128 (2004) 193.
[13] Y. Li, W.J. Meng, S. Swathirajan, S.J. Harris, G.L. Doll, US Patent No. 5,624,769, April 29, (1997).
[14] A. Pozio, R.F. Silva, M. De Francesco, L. Giorgi, Electrochim. Acta 48 (2003) 1543.
[15] M. Rockel, Corrosion behaviour of nickel alloys and high-alloy stainless steel, in: U. Heuβner (Ed.), Nickel Alloys, Marcel Decker Inc., New York, 1998, pp. 44–49.
[16] O.J. Murphy, A. Cisar, E. Clarke, Electrochim. Acta 43/24 (1998) 3829.
[17] D.R. Hodgson, B. May, P.I. Adcock, D.P. Davies, J. Power Sources 96 (2001) 233.
[18] J. Wind, R. Späh, W. Kaiser, G. Böhm, J. Power Sources 105 (2002) 256.
[19] S.J. Lee, C.H. Huang, J.J. Lai, Y.P. Chen, J. Power Sources 131 (2004) 162.
[20] S.J. Lee, C.H. Huang, Y.P. Chen, J. Mater. Process. Technol. 140 (2003) 688.

[21] H. Wang, M.P. Brady, G. Teeter, J.A. Turner, J. Power Sources 138 (2004) 86.
[22] H.P. Feng, C.H. Hsu, J.K. Lu, Y.H. Shy, Mater. Sci. Eng. A 347 (2003) 123.
[23] M.P. Brady, K. Weisbrod, I. Palauskas, R.A. Buchanan, K.L. More, H. Wang, M. Wilson, F. Garzon, L.R. Walker, Scripta Mater. 50 (2004) 1017.
[24] R.F. Silva, D. Franchi, A. Leone, L. Pilloni, A. Masci, A. Pozio, Electrochim. Acta 51 (2006) 3592.
[25] R.F. Silva, A. Pozio, J. Fuel Cell Sci. Technol. 4 (2007) 116.
[26] P. Kinnunen, PhD Thesis, Helsinki University of Technology, 2002.
[27] J.S. Kim, W.H.A. Peelen, K. Hemmes, R.C. Makkus, Corros. Sci. 44 (2002) 635.
[28] D.G. Nam, H.C. Lee, J. Power Sources 170 (2007) 168.
[29] C. Issartel, H. Buscail, E. Caudron, R. Cueff, F. Riffard, S. Perrier, P. Jacquet, M. Lambertin, Corros. Sci. 46 (2004) 2191.